Revista Mexicana de Astronomía y Astrofísica, **48**, 235–242 (2012)

THE EXPANSION OF A STELLAR WIND BUBBLE WITHIN A NON-SINGULAR, STRATIFIED CORE

J. C. Rodríguez-Ramírez and A. C. Raga

Instituto de Ciencias Nucleares
Universidad Nacional Autónoma de México, México

Received 2012 May 30; accepted 2012 June 19

RESUMEN

Estudiamos analíticamente la expansión de una burbuja no radiativa (alimentada por el viento de una estrella masiva) dentro de un medio ambiente con una estratificación de esfera isotérmica autogravitante no singular. Derivamos la ecuación de movimiento para el radio externo de la burbuja (usando las suposiciones del modelo analítico clásico, pero permitiendo la transición apropiada de fuerte a débil para el choque externo). La ecuación del modelo tiene un único parámetro adimensional, que determina si el choque externo se vuelve débil o no. Encontramos que las burbujas de estrellas O en núcleos moleculares estratificados densos (posiblemente asociadas con algunas de las regiones HII ultracompactas observadas) están en el límite de las soluciones de choque fuerte.

ABSTRACT

We study analytically the expansion of a non-radiative bubble (driven by the wind from a massive star) into an environment with a non-singular, self-gravitating isothermal sphere density stratification. We derive the equation of motion for the outer radius of the bubble (using the assumptions of the classical analytic model for expanding bubbles, but allowing the outer shock to have the appropriate strong/weak shock transition). The model equation has a single dimensionless parameter that determines whether or not the outer shock becomes weak. We find that O star bubbles within dense, stratified molecular cloud cores (possibly associated with some of the observed ultracompact HII regions) are in the “strong shock” limit.

Key Words: ISM: evolution — ISM: kinematics and dynamics — stars: formation

1. INTRODUCTION

Compact or ultra-compact HII regions observed at radio wavelengths (see, e.g., the review of Kurtz 2005) are located within dense molecular clouds. These regions have been modeled as the gasdynamic expansion of the high-pressure, photoionized gas into an approximately uniform external medium (Spitzer 1968), or into a stratified medium (Shu et al. 2002; Franco, Tenorio-Tagle, & Bodenheimer 1990). Also, the effect of including the wind from the central, massive star has been included (see, e.g., the review of Cappriotti & Kozminski 2001).

In two recent papers, Raga, Cantó, & Rodríguez (2012a,b) have modified the “classical” analytic models of expanding HII regions and of wind-driven shells (appropriate for compact HII regions with shell-like morphologies, see, e.g. Carral et al. 2002), so as to include the effect of the outer shock becoming weak. These models have the feature of attaining pressure equilibrium with the surrounding environment, a regime which is reached within only $\sim 10^5$ yr by ultra-compact HII regions.

In the present paper, we extend the wind-driven shell model of Raga et al. (2012b) to the case of a stratified environment. In particular, we consider an environment with the density stratification of a non-singular, self-gravitating isothermal sphere.

The picture behind this choice is that one has a star which forms through the gravitational collapse of the central region of a dense, molecular cloud core (with an approximate isothermal sphere stratification). When the stellar wind "turns on", it initially interacts within the material that is still collapsing towards the center of the cloud core. This regime has been studied in detail by González-Avilés et al. (2005).

After a timescale of $\sim 10^4$ yr, the stellar wind has expanded enough to start to interact with the surrounding, still unperturbed region of the molecular cloud core (see, e.g., García-Segura & Franco 1996; Franco et al. 2007). For modelling this regime, we assume that the surrounding cloud core has a non-singular, isothermal sphere density stratification, and that the stellar wind goes through a non-radiative reverse shock, feeding an expanding, hot bubble. This bubble pushes out a shell of swept-up environmental material, and the internal region of this shell is photoionized by the radiation from the central star (therefore corresponding to the ultra-compact HII region, see Raga et al. 2012b).

In the present paper we apply the "thick shell" formalism of Raga et al. (2012a,b) to the problem of a stellar wind bubble expanding within a self-gravitating, non-singular isothermal sphere density stratification. The paper is organized as follows. The approximate form which we use for the environmental stratification is discussed in § 2. The treatment we have done of the division of the wind energy between hot bubble thermal energy and swept-up environment kinetic energy is discussed in § 3. The derivation of the equation of motion for the outer radius of the hot bubble is given in § 4. Approximate, analytic solutions to the model equation are derived in § 5. A comparison between the approximate analytic solutions and an "exact" numerical solution is given in § 6, and a qualitative interpretation of the results is presented in § 7. An application to the parameters relevant for a massive star inside a dense molecular cloud core is given in § 8. Finally, a summary of the work is presented in § 9.

2. THE ENVIRONMENTAL STRATIFICATION

We consider the time-evolution of a wind-driven bubble within a non-singular, self-gravitating, isothermal sphere. In order to obtain an analytic model, we approximate the non-singular solutions to the Lane-Emden equation with the analytic density profile:

$$\rho_e(R) = \frac{\rho_0}{1 + (R/r_0)^2}\,, \tag{1}$$

where

$$r_0 = \sqrt{\frac{3c_0^2}{2\pi G \rho_0}} \tag{2}$$

is the core radius, c_0 is the isothermal sound speed and r_0 the core radius of the isothermal sphere, G is the gravitational constant and R is the spherical radius. While this approximate form gives substantial errors in the density at large distances (see Natarajan & Lynden-Bell 1997), it does have the correct, $\propto R^{-2}$ asymptotic dependence for $R \gg r_0$.

In principle, it would be possible to use the more complex approximation proposed by Natarajan & Lynden-Bell (1997) for the density stratification. However, for a first exploration of the proposed problem, the simpler density law given by equation (1) appears to be appropriate.

3. THE ENERGY OF THE BUBBLE

At $t = 0$, a stellar wind of constant mass loss rate $\dot{M}$ and terminal wind velocity v_w is suddenly "turned on" at the center of the stratified environmental density distribution given by equation (1). We assume that the stellar wind goes through a "reverse shock" with a spherical radius much smaller than the size of the wind-driven bubble. The hot bubble pushes out the environmental material, which is piled up into a thin shell. Following the "classical" derivation (see, e.g., Dyson & Williams 1980), we assume that the shock driven into the environment is isothermal, which is a reasonable approximation in the regime in which this outer shock has velocities of less than a few hundred km s^{-1}.

The kinetic energy E injected by the wind is then converted into thermal energy of the bubble+kinetic energy of the thin shell:

$$E = \frac{\dot{M} v_w^2 t}{2} = \frac{3}{2} PV + \frac{M_s v_s^2}{2}\,, \tag{3}$$

where t is the time, $\dot{M}$ is the stellar mass loss rate, v_w the terminal wind velocity, P the pressure of the bubble (assumed to be uniform), M_s the mass within the thin shell, v_s the outward velocity of the thin shell and $V = (4\pi/3)R^3$ is the volume of the hot bubble, with R being its outer radius.

The swept-up mass M_s within the thin shell is equal to the mass of the environmental density stratification within a radius R:

$$M_s = 4\pi \int_0^R {R'}^2 \rho_e(R')\, dR'\,, \tag{4}$$

where we have neglected the width of the thin shell, and $\rho_e(R)$ is given by equation (1).

We now assume that the shock driven by the expansion into the environment is a strong, isothermal shock. Therefore, the compression at the shock is very large, and the shock velocity follows the relation

$$v_s \approx \dot{R}\,, \tag{5}$$

where $\dot{R}$ is the expansion velocity of the outer radius of the hot bubble. For an isothermal shock, the post-shock pressure is given by:

$$P_{ps} = \rho_e(R) v_s^2\,, \tag{6}$$

which is valid for a general (i.e., not necessarily strong) shock.

Finally, setting $P_{ps} = P$ (i.e., the post-shock pressure equal to the pressure of the hot bubble), from equations (3–6) we obtain:

$$P = \frac{\dot{M} v_w^2 t}{4\pi R^3} f(R), \tag{7}$$

with

$$f(R) = \left\{1 + [R - r_0 \tan^{-1}(R/r_0)](r_0^2 + R^2)/R^3\right\}^{-1}\,. \tag{8}$$

Equation (7) gives us the pressure P of the hot bubble as a function of t and R (the evolutionary time and the outer radius of the bubble, respectively).

Even though this relation has been obtained assuming that the isothermal shock driven into the undisturbed environment is strong, we will assume that it is also approximately valid in the regime in which the shock is no longer strong. This inconsistency in the derivation of the model equation is at the heart of the "thick shell formalism" of Raga et al. (2012a,b).

4. THE MODEL EQUATION

We now consider that the outer boundary R of the hot bubble acts like a plane piston which pushes out a shock wave into the surrounding environment. Using the fact that the velocity of the post-shock material relative to an isothermal shock is $v_{ps} = c_0^2/v_s$, and that the velocity of the shock is $v_s = \dot{R} + v_{ps}$ (where $\dot{R} = dR/dt$ is the velocity of the piston), we obtain the relation

$$\frac{dR}{dt} = v_s - \frac{c_0^2}{v_s}\,, \tag{9}$$

from which one can recover equation (5) for the strong shock, $v_s \gg c_0$ case. Combining this equation with equations (6–7), we then obtain a differential equation for the outer radius R of the hot bubble:

$$\frac{dr}{d\tau} = \sigma\tau^{1/2} f^{1/2}(r)\left(\frac{1+r^2}{r^3}\right)^{1/2} - \frac{1}{\sigma\tau^{1/2} f^{1/2}(r)}\left(\frac{r^3}{1+r^2}\right)^{1/2}, \tag{10}$$

with

$$f(r) = \left[1 + (r - \tan^{-1} r)\left(\frac{1+r^2}{r^3}\right)\right]^{-1}, \tag{11}$$

where $r \equiv R/r_0$, $\tau \equiv tc_0/r_0$ and

$$\sigma \equiv \sqrt{\frac{\dot{M} v_w^2}{4\pi\rho_0 r_0^2 c_0^3}}\,. \tag{12}$$

Let us note that the $f(r)$ is only a weak function of r, with $f(0) = 3/4$ and $f(\infty) = 1/2$. In the following section we will use this fact in order to derive an approximate analytic solution of equation (10).

If one specifies a value for the dimensionless parameter σ (given by equation 12), equation (10) can be integrated numerically in a straightforward way with the boundary condition $r \to 0$ for $\tau \to 0$. Results of such an integration (carried out with a fourth-order Runge-Kutta algorithm) are shown for $\sigma = 10$, 3, 1, 0.5, 0.1 and 0.05 in Figure 1. We also derive approximate analytic solutions to our model (equation 10), which are described in the following section. The resulting time-evolutions are discussed in § 6.

5. ANALYTIC SOLUTIONS

5.1. *The $\sigma \gg 1$ case*

For $\sigma \gg 1$, we keep only the first term on the right hand side of equation (10), so that we have:

$$\frac{dr}{d\tau} = \sigma\tau^{1/2} f^{1/2}(r)\left(\frac{1+r^2}{r^3}\right)^{1/2}. \tag{13}$$

This equation of motion for the outer radius of the hot bubble corresponds to a case in which the shock driven into the surrounding ISM is always strong.

With the boundary condition $r \to 0$ for $\tau \to 0$, this equation can be integrated formally to obtain:

$$\frac{2}{3}\sigma\tau'^{3/2}\Big|_{\tau_0}^{\tau} = \left[f^{-1/2}(r')\int\left(\frac{r'^3}{1+r'^2}\right)^{1/2} dr'\right]\Bigg|_{r_0}^{r}. \tag{14}$$

To derive this equation, we take out $f(r)$ from the radial integral, since $f(r)$ is a weak function of r (see § 2). Even with this simplification, the radial integral of equation (14) does not have an analytic solution. We therefore derive an approximate solution, which is calculated as follows.

Let us call $h(r)$ the integrand of equation (14). We then consider three Taylor series expansions:

i. Writing $h(r) = r^{3/2}(1+r^2)^{-1/2}$, an expansion of $(1+r^2)^{-1/2}$ to first order in r^2 around $r = 0$ gives:

$$h_0(r) = r^{3/2} - \frac{1}{2}r^{7/2}\,, \tag{15}$$

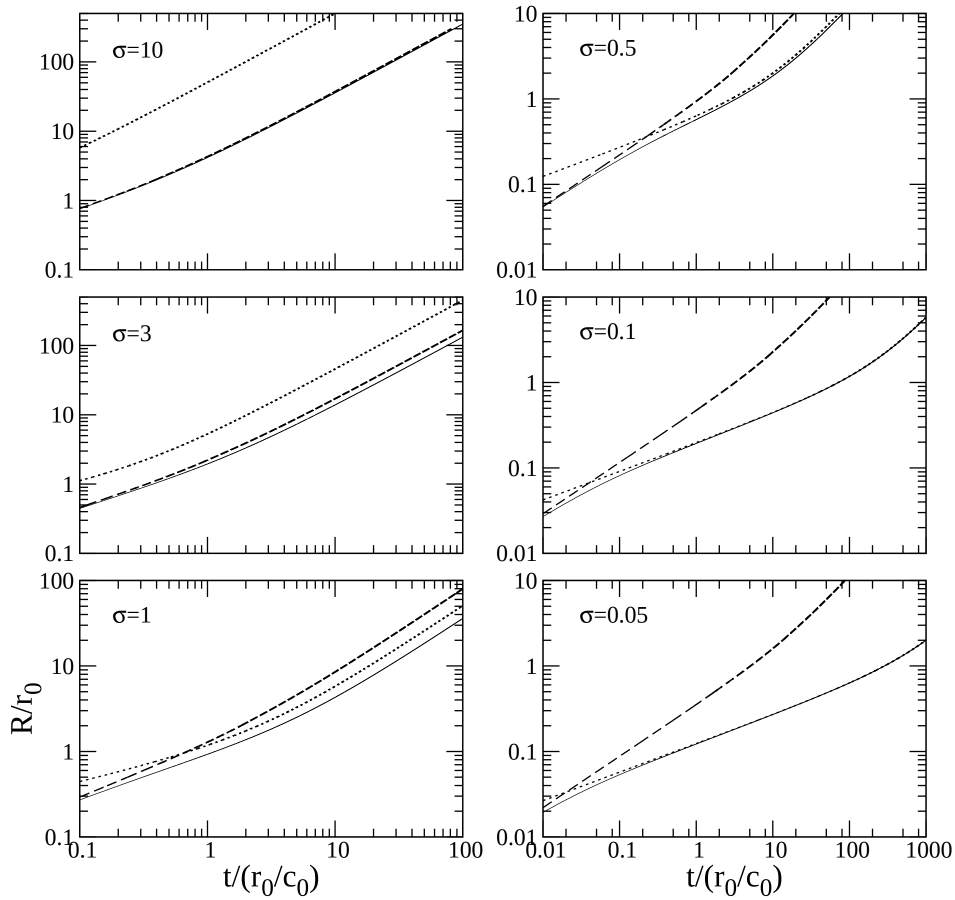

Fig. 1. Numerical solutions (solid lines), high σ analytic solutions (dashed lines) and low σ analytic solutions (dotted lines) for the radius of the expanding bubble as a function of time. The panels are labeled with the values of σ for which the solutions were calculated.

ii. An expansion of $h(r)$ to second order in $r-1$ around $r=1$ gives:

$$h_1(r) = \frac{1}{4\sqrt{2}}\left(6r - r^2 - 1\right), \qquad (16)$$

iii. Writing $h(r) = r^{1/2}(1+1/r^2)^{-1/2}$, an expansion of $(1+1/r^2)^{-1/2}$ to first order in $1/r^2$ around $1/r = 0$ gives:

$$h_\infty(r) = r^{1/2} - \frac{1}{2}r^{-3/2}. \qquad (17)$$

We note that these expansions of the integrand satisfy $h_0(1/2) = h_1(1/2)$ and $h_1(2) = h_\infty(2)$.

So, in order to solve the radial integral of equation (14) we set $h(r) = h_0(r)$ for $0 \le r < 1/2$, $h(r) = h_1(r)$ for $1/2 \le r < 2$ and $h(r) = h_\infty(r)$ for $2 \le r$. The resulting integrals have trivial analytic solutions, giving a solution for the dimensionless time τ as a function of the dimensionless radius r (of the hot bubble) of the form:

$$\tau_0^{(0)}(r) = \left[\frac{3}{2\sigma} I_0(r)\right]^{2/3}, \quad \text{for} \quad r \le 1/2, \qquad (18)$$

$$\tau_1^{(0)}(r) = \left[\tau_0^{3/2}(\tfrac{1}{2}) + \frac{3}{2\sigma}\left(I_1(r) - I_1(\tfrac{1}{2})\right)\right]^{2/3}, \qquad (19)$$

for $1/2 < r \le 2$,

$$\tau_\infty^{(0)}(r) = \left[\tau_1^{3/2}(2) + \frac{3}{2\sigma}\left(I_\infty(r) - I_\infty(2)\right)\right]^{2/3}, \qquad (20)$$

for $2 \le r$, with

$$I_0^{(0)}(r) \equiv \left(\frac{2}{5}r^{5/2} - \frac{1}{9}r^{9/2}\right) f^{-1/2}(r), \qquad (21)$$

$$I_1^{(0)}(r) \equiv \frac{1}{4\sqrt{2}}\left(-r + 3r^2 - \frac{r^3}{3}\right) f^{-1/2}(r), \qquad (22)$$

$$I_\infty^{(0)}(r) \equiv \left(\frac{2}{3}r^{3/2} + r^{-1/2}\right) f^{-1/2}(r). \qquad (23)$$

5.2. *The $\sigma \ll 1$ case*

In the $\sigma \ll 1$ limit, as the evolutionary time increases the second term on the right hand side of equation (10) becomes comparable to the first term (which diverges at $\tau = 0$). From then on, the time evolution of the hot bubble enters a quasi-static regime, in which it expands in approximate pressure equilibrium with the surrounding environment as more material is fed into the bubble by the stellar wind. This quasistatic regime is always found at large evolutionary times in the expansion of a wind-driven bubble into a uniform environment (see Raga et al. 2012b).

From the approximate balance between the two terms on the right of equation (10), one obtains:

$$\tau(r) = \frac{1}{\sigma^2}\left[\frac{r(1+2r^2)}{1+r^2} - \arctan r\right] . \qquad (24)$$

5.3. *The $\sigma \sim 1$ case.*

In order to model the transition between the strong and weak shock regimes, we calculate a perturbative solution to equation (10). This is done considering the second term on the right hand side of equation (10), as a small perturbation of the left term. We first re-write equation (10) in the form

$$\frac{d\tau}{dr} = \frac{\mu}{\tau^{1/2} f^{1/2}(r)}\left(\frac{r^3}{1+r^2}\right)^{1/2} + \frac{\lambda}{\tau^{3/2} f^{3/2}(r)}\left(\frac{r^3}{1+r^2}\right)^{3/2} , \qquad (25)$$

where we have defined the parameters $\mu \equiv 1/\sigma$, and $\lambda \equiv 1/\sigma^3$. Note that $\lambda < \mu$ for $\sigma > 1$. We then assume that the solution has the form $\tau = \tau^{(0)} + \lambda\tau^{(1)} + ... + \lambda^n \tau^{(n)}$, with n its perturbative degree. We calculate only the first order approximation, so that we have:

$$\tau(r) = \tau^{(0)}(r) + \lambda\tau^{(1)}(r) . \qquad (26)$$

From equations (26) and (25) we then obtain the system of differential equations:

$$\frac{d\tau^{(0)}}{dr} = \frac{\mu}{{\tau^{(0)}}^{1/2} f^{1/2}(r)}\left(\frac{r^3}{1+r^2}\right)^{1/2} , \qquad (27)$$

$$\frac{d\tau^{(1)}}{dr} = q(r) - p(r)\tau^{(1)} , \qquad (28)$$

with

$$p(r) \equiv \frac{\mu}{2 f^{1/2}(r)\, {\tau^{(0)}}^{3/2}}\left(\frac{r^3}{1+r^2}\right)^{1/2} , \qquad (29)$$

$$q(r) \equiv \frac{1}{f^{3/2}(r)\, {\tau^{(0)}}^{3/2}}\left(\frac{r^3}{1+r^2}\right)^{3/2} . \qquad (30)$$

Equation (27) is the strong shock model and its solution is given in § 5.1. This solution is used to solve equation (28), giving:

$$\tau^{(1)}(r) = \frac{1}{\eta(r)}\int_{r_0}^{r} \eta(r')q(r')dr' , \qquad (31)$$

where $\eta(r)$ is the integrating factor of equation (28):

$$\eta(r) = \exp\left\{\int p(r)\, dr\right\} . \qquad (32)$$

In order to find analytic solutions, we have divided the radial domain as we have done in § 5.1, obtaining:

$$\tau_0^{(1)}(r) = \frac{2\sigma}{3} I_0^{(1)}(r) , \qquad (33)$$

$$\tau_1^{(1)}(r) = \frac{2\sigma}{3}\frac{I_1^{(1)}(r) - I_1^{(1)}(1/2)}{\left[A_1 + I_1^{(0)}(r) f^{1/2}(r)\right]^{1/3}} , \qquad (34)$$

$$\tau_\infty^{(1)}(r) = \frac{2\sigma}{3}\frac{I_\infty^{(1)}(r) - I_\infty^{(1)}(2)}{\left[A_\infty + I_\infty^{(0)}(r) f^{1/2}(r)\right]^{1/3}} , \qquad (35)$$

with

$$I_0^{(1)}(r) \equiv \frac{15}{23} r^3 f^{-1}(r) , \qquad (36)$$

$$I_1^{(1)}(r) \equiv -\frac{2}{33}r^3 + \frac{12}{11}r^2 - \frac{64}{77}r , \qquad (37)$$

$$I_\infty^{(1)}(r) \equiv \left[(3/2)^{-1/3} r^{3/2} - (3/2)^{2/3} A_\infty \ln r - \frac{1}{2}(3/2)^{5/3} A_\infty r^{-2}\right] f^{-1}(r) , \qquad (38)$$

$$A_1 \equiv \left[\frac{2\sigma}{3}\tau_0^{3/2}(1/2) - I_1^{(0)}(1/2)\right] f^{1/2}(r) , \qquad (39)$$

$$A_\infty \equiv \left[\frac{2\sigma}{3}\tau_1^{3/2}(2) - I_\infty^{(0)}(2)\right] f^{1/2}(r) . \qquad (40)$$

We build our final solution $\tau_{0,1,\infty}$ by employing equation (26) within each radial domain. In Figure 2 we show the r vs. τ solutions obtained with this perturbative method, and compare them with a numerical integration of the full model equation (equation 10). We show the solutions for $\sigma = 2, 1$, and 0.1, which are described in more detail in the following section.

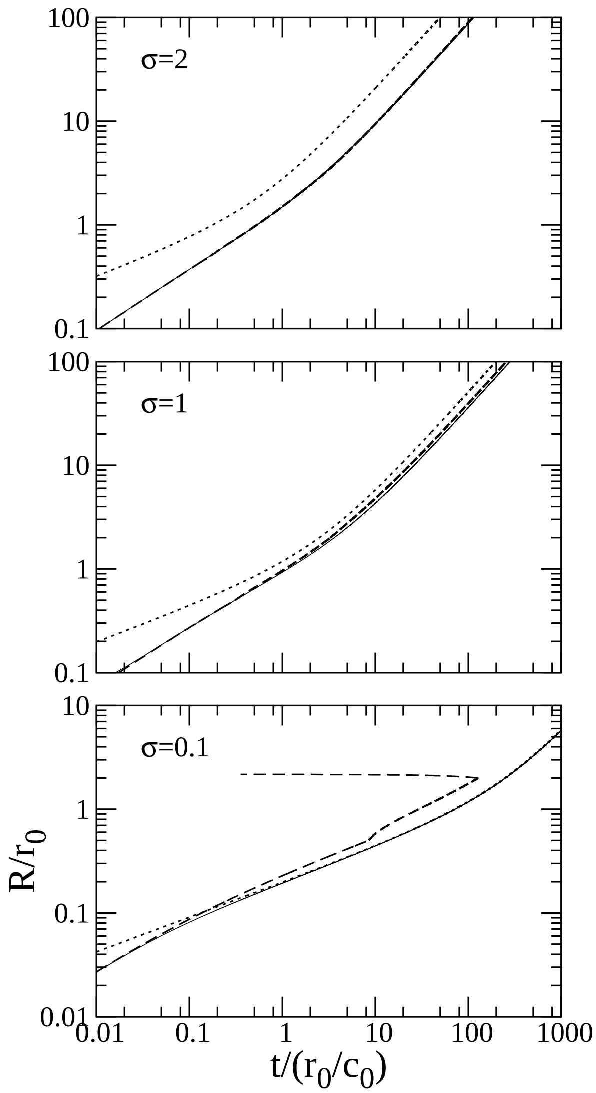

Fig. 2. Numerical solutions (solid lines), perturbative analytic solutions (dashed lines) and low σ analytic solutions (dotted lines) for the radius of the expanding bubble as a function of time. The panels are labeled with the values of σ for which the solutions were calculated.

6. COMPARISON BETWEEN THE ANALYTIC AND NUMERICAL SOLUTIONS

In Figure 1, we show the hot bubble radius as a function of time obtained for different σ values from:

i. Solid lines → a numerical integration of equation (10),

ii. Dashed lines → the large σ analytic solution (equations 18–20),

iii. Dotted lines → the small σ analytic solution (equation 24).

From this figure, it is clear that for $\sigma = 10$ (top left frame) the large σ analytic solution (equations 18–20) basically coincides with the full, numerical solution. Also, we see that for $\sigma = 0.05$ the numerical solution coincides with the small σ analytic solution (equation 24) except during its very early evolution (with $\tau, r < 0.1$).

We also see that for $\sigma = 1$, both analytic solutions fail to reproduce the full (i.e., numerical) integral of the equation of motion (equation 10). However, for $\sigma = 3$ the large σ analytic solution does not differ in a substantial way from the full solution, and for $\sigma = 0.5$ the small σ solution reproduces well the full solution (except for early evolutionary times). Therefore, there is only a limited parameter range $0.5 < \sigma < 3$ for which we do not have an analytic solution that describes (in an approximate way) the behavior of the full solution for the expansion of the hot bubble as a function of time.

In Figure 2 we show a comparison between the numerical solutions to the full model equation (equation 10) and the high σ analytic, perturbative solution of § 5.3. From this figure, we see that the perturbative solution works well for $\sigma \geq 1$. However, for $\sigma < 1$, the perturbative solution is a good approximation to the full (numerical) solution only for $t \ll 1$. In spite of this, it gives an improvement for the small σ regime, because neither the zero order solution nor the balance solution reproduce the full numerical solution at early evolutionary times (as one can see from Figure 1).

In summary, the perturbative analytic solution reproduces very well the numerical solution for $\sigma \geq 1$. For $\sigma \leq 1$ a good analytic solution can be constructed by choosing the minimum value of r (at a given τ) between the perturbative and the balance solutions (therefore, choosing the perturbative solution for small values of τ, and the balance solution for large τ, as can be seen from the bottom panel of Figure 2).

7. INTERPRETATION OF THE SOLUTIONS

The evolution of the expanding bubble has two regimes:

i. For $R < r_0$ (where R is the outer radius of the bubble and r_0 is the core radius of the environmental stratification, see equation 2) the expansion is similar to the one of a wind-driven bubble within a constant density environment. This evolution has been described in detail by Raga et al. (2012b),

ii. For $R > r_0$, the bubble expands into an environment with a stratification that approaches a $\rho \propto R^{-2}$ law.

This second regime was studied analytically by Dyson (1989), and our large σ solution (equations 18–20) coincide with Dyson's solutions at large evolutionary times (Dyson 1989 did not explore the weak shock regime).

Our new solutions can be understood in a qualitative way as follows. Raga et al. (2012b, their equation 7) showed that the shock pushed out by a wind-driven bubble expanding into a uniform environment becomes weak when it reaches a radius

$$R_0 = \sqrt{\frac{3\dot{M}v_w^2}{16\pi\rho_0 c_0^3}}\,. \tag{41}$$

Combining this equation with the definition of σ (equation 12), we obtain that $\sigma = \sqrt{4/3}R_0/r_0$ (where r_0 is the core radius of the environmental stratification, given by equation 2). Therefore, for low values of σ, the expanding bubble slows down to produce a weak outer shock within the approximately constant density core of the environmental stratification, and the shock remains weak during all of the subsequent evolution.

Conversely, for large values of σ, the expanding bubble reaches the $\rho \propto r^{-2}$ region (of the environmental density stratification) with a strong outer shock, and then the shock remains strong during the rest of the expansion.

From equation (20), we see that in the asymptotic regime of large evolutionary times, the high σ solution gives a constant expansion velocity:

$$v_\infty = \sigma^{2/3} c_0\,. \tag{42}$$

For the $\sigma \ll 1$ regime, the expansion also reaches an asymptotic expansion velocity. Taking the $r \to \infty$ limit in equation (24), we see that the asymptotic velocity now is:

$$v_\infty = \frac{\sigma^2}{2} c_0\,. \tag{43}$$

The assumption we have made of uniform pressure within the hot bubble is only valid if $v_\infty \ll v_w$, so that in order to apply our model to specific cases one should check whether or not this condition is met (using the equations 42 or 43 depending on the value of σ).

8. THE VALUES OF THE σ PARAMETER

If we combine equation (2) for the core radius and equation (12), we obtain:

$$\sigma = \sqrt{\frac{G\dot{M}v_w^2}{6c_0^5}} = 112.7\left(\frac{\dot{M}}{2\times10^{-6}\ M_\odot\ \mathrm{yr}^{-1}}\right)^{1/2} \times\left(\frac{v_w}{3000\,\mathrm{km\,s^{-1}}}\right)\left(\frac{1\,\mathrm{km\,s^{-1}}}{c_0}\right)^{5/2}\,, \tag{44}$$

where the second equality gives the value of σ for the parameters of an O4 star. If we consider the wind parameters for an O7 star ($\dot{M} \approx 4.5\times10^{-7}\ M_\odot\ \mathrm{yr}^{-1}$ and $v_w \approx 2500$ km s^{-1}, see Sternberg, Hoffman, & Pauldrach 2003), we obtain $\sigma \approx 45$.

If we use the new mass loss rate estimates of Marcolino et al. (2009), for an O9 star we have $\dot{M} \approx 2\times10^{-9}\ M_\odot\ \mathrm{yr}^{-1}$ and $v_w \approx 2000$ km s^{-1}. With these parameters, from equation (44) we obtain $\sigma \approx 2.4$.

Therefore, for the case of an O star driving a wind into a molecular cloud core with a non-singular, self-gravitating isothermal sphere stratification, the resulting hot bubble is always in the "strong outer shock" regime. This is the regime described by our "high σ" analytic solution (equations 18–20).

Finally, if we insert $\sigma \sim 100$ and $c_0 \sim 1$ km s^{-1} in equation (42), we obtain $v_\infty \sim 20$ km s^{-1}, so that the bubble of an O star (with $v_w \sim 1000$ km s^{-1}) inside a self-gravitating sphere expands at velocities ∼1 to 2 orders of magnitude lower than the wind velocity. Therefore, the approximation of uniform pressure across the bubble (necessary for deriving our model) is valid for late enough evolutionary times.

9. CONCLUSIONS

We have developed an analytic model for the expansion of a wind bubble blown by a massive star embedded within an environment with a non-singular, self-gravitating sphere. The model is based on the classical assumption that the wind goes through a "reverse shock" close to the source, that the shocked gas produces a hot bubble of uniform pressure, and that the environment pushed by the bubble is swept up into a thin shell (see, e.g., the book of Dyson & Williams 1980). Our assumptions differ from the classical model in that we allow for the (isothermal) outer shock to have the general jump relations (deviating from the strong shock regime).

We derive a model equation which depends on a dimensionless parameter σ (see equation 12). For $\sigma \gg 1$, the bubble pushes out a strong shock during all of the expansion. For $\sigma \ll 1$, the outer shock rapidly becomes weak, and the subsequent evolution of the bubble is in a regime of approximate pressure balance with the surrounding environment (the expansion being maintained by the injection of new material by the stellar wind). We find approximate analytic solutions for both the high and low σ regimes, and give numerical integrations of the model equation for $\sigma \sim 1$. Additionally, we derive a more complex analytic solution appropriate for the $\sigma \sim 1$ regime (see § 5.3).

If we insert parameters appropriate for an O star ($\dot{M} \sim 10^{-6}\ M_{\odot}\ \mathrm{yr}^{-1}$, $v_w \sim 3000$ km s^{-1}) within a molecular cloud core (with isothermal sound speed $c_0 \sim 1$ km s^{-1}), we obtain $\sigma \sim 100$. Therefore, the expansion clearly lies in the regime in which the outer shock is always strong.

For example, if we consider a density of H nuclei of $\approx 10^7$ cm^{-3} for the central core of the molecular clump (in which the wind source is embedded), from equation (2) we obtain a $r_0 = 6 \times 10^{16}$ cm core radius. The wind bubble would then expand following a $R \propto t^{5/3}$ law (see equation 18) until a time $t \sim r_0/c_0 \approx 2 \times 10^4$ yr (corresponding to a dimensionless time $\tau = 1$, see Figure 1). For $t > r_0/c_0$, the expansion enters a linear regime, with a constant velocity approximately $v_\infty \approx 20$ km s^{-1} (see equation 42).

In this way, our model can be used to obtain the expansion velocity of wind-driven shells. Such predictions could be used to interpret future radio or millimetric observations of either the radial velocity (through H recombination line measurements) or proper motion (from maps at different epochs) measurements of the expansion of compact HII regions.

Finally, we find that the "low σ" regime (in which the wind bubble expands in an approximate bubble/environment pressure equilibrium, see equation 24) is not applicable to the case of massive stars embedded in stratified molecular cloud cores. This regime might be relevant for other astrophysical situations (e.g., to the case of the winds from massive stars embedded in a pre-existing, coronal gas bubble).

We acknowledge support from Conacyt grants 61547, 101356 and 101975.

REFERENCES

Capriotti, E. R., & Kozminski, J. F. 2001, PASP, 113, 677

Carral, P., Kurtz, S. E., Rodríguez, L. F., Menten, K., Cantó, J., & Arceo, R. 2002, AJ, 123, 2574

Dyson, J. E. 1989, Lectures Notes in Physics, 350, 137

Dyson, J. E., & Williams, D. A. 1980, The Physics of the Interstellar Medium (Manchester: Manchester Univ. Press)

Franco, J., García-Segura, G., Kurtz, S. E., & Arthur, S. J. 2007, ApJ, 660, 1296

Franco, J., Tenorio-Tagle, G., & Bodenheimer, P. 1990, ApJ, 349, 126

García-Segura, G., & Franco, J. 1996, ApJ, 469, 171

González-Avilés, M., Lizano, S., & Raga, A. C. 2005, ApJ, 621, 359

Kurtz, S. 2005, IAU Symp. 227, Massive Star Birth: A Crossroads of Astrophysics, ed. R. Cesaroni, M. Felli, E. Churchwell, & M. Walmsley (Cambridge: Cambridge Univ. Press), 111

Marcolino, W. L. F., Bouret, J.-C., Martins, F., Hillier, D. J., Lanz, T., & Escolano, C. 2009, A&A, 498, 837

Natarajan, P., & Lynden-Bell, D. 1997, MNRAS, 286, 268

Raga, A. C., Cantó, J., & Rodríguez, L. F. 2012a, MNRAS, 419, L39

__________. 2012b, RevMexAA, 48, 199

Shu, F. H., Lizano, S., Galli, D., Cantó, J., & Laughlin, G. 2002, ApJ, 580, 969

Spitzer, L. 1968, Diffuse Matter in Space (New York: Interscience)

Sternberg, A., Hoffman, T. L., & Pauldrach, A. W. A. 2003, ApJ, 599, 1333

J. C. Rodríguez-Ramírez and A. C. Raga: Instituto de Ciencias Nucleares, Universidad Nacional Autónoma de México, Apdo. Postal 70-543, 04510 D. F., México (juan.rodriguez, raga@nucleares.unam.mx)